ISTITUTO NAZIONALE DI FISICA NUCLEARE

Sezione di Genova

INFN/TC-03/13
3 Settembre 2003

R&D MECHANICAL STUDIES OF THE PHOTON DETECTOR MICROCELLS AND MODULES FOR THE EUSO EXPERIMENT

M. Ameri[1], F. Cadoux[2], R. Cereseto[1], G. Corti[3], S. Cuneo[1*], P. Musico[1], E. Pace[3], A. Petrolini[1], P. Pollovio[1], F. Pratolongo[1], F. Siccardi[1], A. Vinci[1]

[1)] *INFN-Sezione di Genova, Dip. Fisica Università di Genova, I-16143 Genova, Italy*
[2)] *LAPP, Annecy, France*
[3)] *Dip. Astronomia e Scienza dello Spazio, Universita' di Firenze, I - 50125, Italy*

Abstract

During the phase "A" of the EUSO experiment [5),6)], extensive R&D studies have been done to optimise the mechanical arrangement of the photon multipliers on the focal surface. The activity has been focused on micro-cell and photon detector module sub-assemblies, the modular units that should tessellate the focal surface of the instrument. Alternative solutions have been investigated, simulations have been performed, prototypes built and tested. All that activity allowed to check the compliance of several features with the space environment, thus identifying those that could be applied in the final design.

Published by ***SIS–Pubblicazioni***
Laboratori Nazionali di Frascati

* Corresponding author. E-mail: stefano.cuneo@ge.infn.it

1. THE MICRO-CELL SUB-ASSEMBLY

1.1 General features

The base-board, made of flame retardant FR-4 glass epoxy laminate, is secured to the PD module supporting base-plate through 4 x M2.5 stainless steel screws. If necessary, for any positioning and/or thermal reason, up to 4 x ϕ2 mm dowel pins (on the corners) could be added, still in compliance with the present layout of electronics components and paths. Fig. 1 describes base-board mechanical outline, as it has been specified to the supplier of the first batch of prototypes. A further study showed that with

- standard printed circuit board manufacturing accuracy (± 0.1 mm);
- maximum MAPMT side length limited to 25.7 mm (instead of the standard 25.7±0.3 mm declared by the manufacturer);
- 0.5 mm as minimum installation clearance between neighbouring MAPMTs, even in the worst condition;

micro-cell assembly side length could be limited to 52.9 mm, instead of the 53.1 specified for the prototypes. That would slightly help to reduce detector dead area.

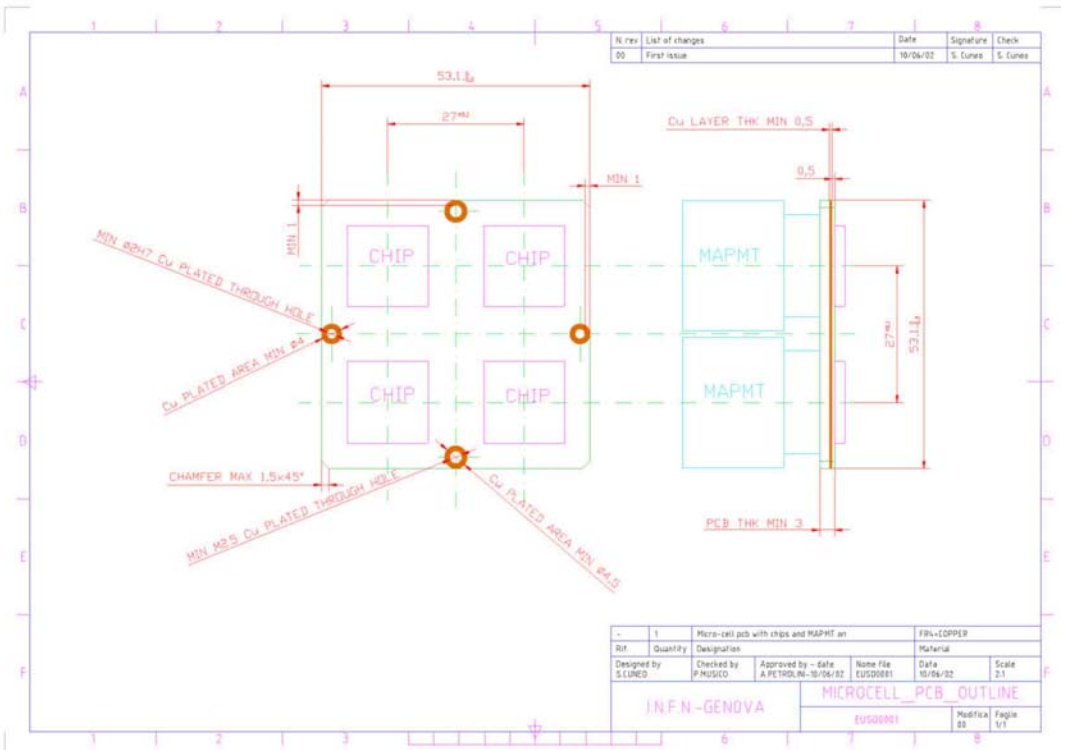

FIG. 1: base-board mechanical layout

Screws are equipped with cylindrical hollow spacers, aluminium made, ϕ5 mm, so that room enough (15 mm high) is available between the base-board and the PD module base-plate to allow the routing of the services. Those spacers let the screw to base-board and

screw to module base-plate joints behave as a fully restrained ones, improving momentum transfer and reducing the stress. Furthermore, they contribute to conductive heat transfer. Spacers with different height could allow to orient the micro-cell but, given the integration complexity it would introduce, that should be definitely considered as a last chance.
Screws and pins fit into holes drilled into the base-board. They also act as thermally conductive bridges to drain to the PD module the heat generated on the base-board. The location of the holes on the base-board is a compromise between the structural requirements and electrical layout.
The base-board present thickness is 4 mm. This might be slightly reduced, without compromising the structural strength. The study for thickness (and, therefore, mass) reduction will be carried as soon as more detailed information and boundary conditions will be available.
The thick base-board integrates a copper layer, 0.5 mm thick, to help to convey the heat to screws, pins and, if necessary, other dedicated heat bridges. To ensure that the mechanical resistance and electrical contacts are kept all life long, the spaces between MAPMTs, between MAPMTs and the BGA sockets, and between BGA sockets and base-board must be potted with an appropriate resin. Presently, NASA-compliant Dow Corning DC-93500 silicone low temperature curing resin has been assumed as baseline potting compound, after the experience on a similar application for the AMS experiment.

1.2 Micro-cell thermal and structural analysis

A preliminary FEA simulation of the base-board has been performed, modelling the base-board with its links to the PD module and considering the MAPMTs as added masses.
A thermal analysis has been performed on a simplified model, where a 4 mm thick FR-4 baseboard with a 0.5 mm thick copper layer inside is thermally linked, via 8xΦ2.5x15 mm stainless steel screws, to a cold pit at 13°C. An uniformly distributed power of 0.27 W, close the actual value expected in operation, entered the base-board through the face on the links side. The results (see Fig. 2) showed that copper layer works well, provided that it is properly linked to the screws, and requires a temperature drop of 5.7°C to drain away the heat.

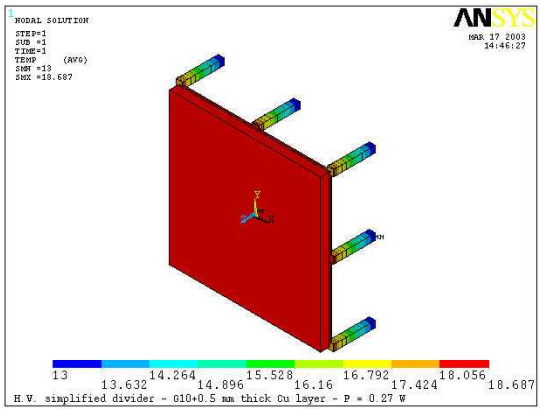

FIG. 2: micro-cell temp.profile with 0.27 W on, screws ends at 13°C and conduction only

The modal analysis of a 5 mm thick base-board, fastened through 4xM2.5x15 stainless steel screws, with an overall mass of 212 gr, has determined the following modal

frequencies: 716, 872, 1259, 1801, 1878 Hz.
Then a random vibration analysis has been performed with the input spectrum NASA suggest for acceptance of items whose mass at launch is below 23 Kg [1] (see Fig 3/a).
Such spectrum of acceleration is equivalent to 6.9 g RMS. A standard damping ratio of 2.5% has been assumed, constant throughout the frequency range. The calculated response of the system, when the excitation is parallel to the base-board plane, showed a sharp peak

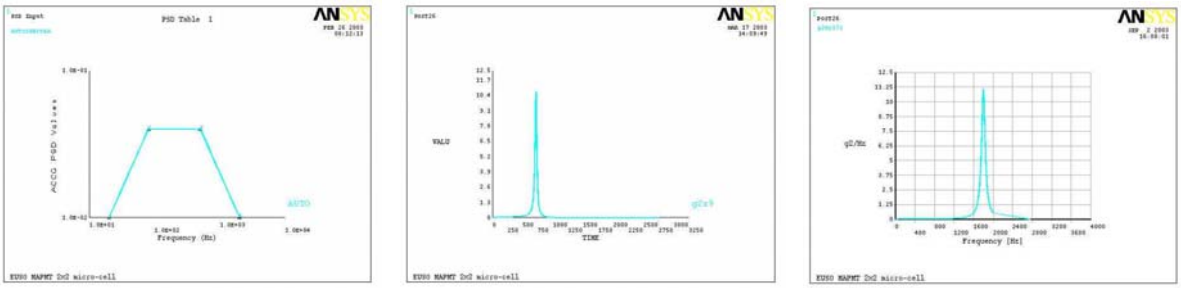

FIG. 3/a: acceptance spectrum equivalent to 6.9 gRMS
FIG. 3/b: response spectrum along X or Y, equivalent to 25 gRMS
FIG. 3/c: response spectrum along Z, equivalent to 38.6 gRMS

in correspondence of the first modal frequency (see Fig. 3/b), with an integral value of 25 g RMS. As a matter of fact, the first mode is a base-board rigid translation due to the bending of the screws. The calculated response of the system, when the excitation is orthogonal to the base-board plane, showed a sharp peak in correspondence of the fifth modal frequency, with an integral value of 38.6 g RMS (see Fig. 3/c). That result is consistent with the fifth modal shape.
The static analysis performed with the above acceleration combined in a load vector (ax,ay,az)=(25g,25g,38g) correctly showed the screws working as fully constrained beams, with the most stressed points at their ends (see Fig. 4). Von Mises' equivalent stress in those points is about 152 MPa, that shouldn't be of great concern neither for the screws nor for the base-board. However, the tests on the vibrating table should confirm

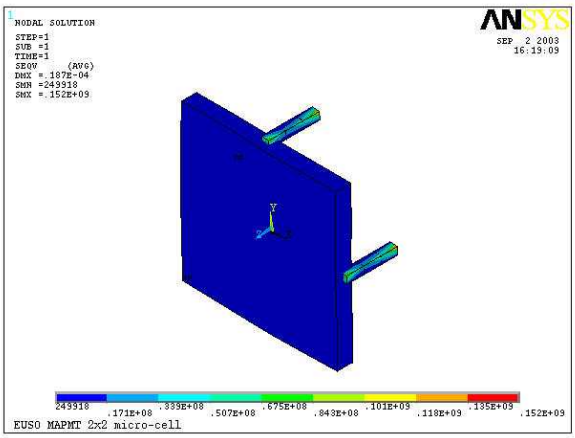

FIG. 4: Von Mises' equivalent stress under (25g,25g,38g), in [N/m2]

that and, possibly, identify the ultimate strength limit of the system. As presently designed, the simulations showed a rather stiff and robust system, but with a rather high response to random vibration. Therefore it is advisable an optimisation phase.

1.3 Laboratory tests

Given the concerns raised by some experts on the effectiveness and reliability of M2 screws, and being rather difficult to fit larger screws in the base-board layout, a test campaign has been started to validate the current design.
As first approach, an M2.5 stainless steel screw have been tightened on a 5 mm thick FR-4 board and submitted to a constant traction force of 110 N, that is approximately 6 times the maximum expected stress under a 38g acceleration parallel to the screw axis, as shown in the RVA analysis, with a 212 gr micro-cell. After 8 months, there was no evidence of damage neither of the base-board, nor of the screw.
Then, M2 stainless steel screws have been tightened to rupture onto a 4.5 mm-thick G10 board (including a 0.5 mm-thick copper layer inside), by means of a dynamometric screwdriver. All the 5 screws tested broke at a torque ranging from 60 to 65 cNm
A batch of base-board prototypes, 4 mm thick with a 0.5 mm thick copper layer inside, has been manufactured to be used in laboratory tests, and equipped with BGA sockets (see Fig. 5/a and 5/b). Due to a manufacturing error, those boards featured 4xM2 holes, instead of the specified 4xM2.5; dummy, expendable, MAPMTs have been procured; then a prototype reasonably close to the designed micro- cell has been set up.

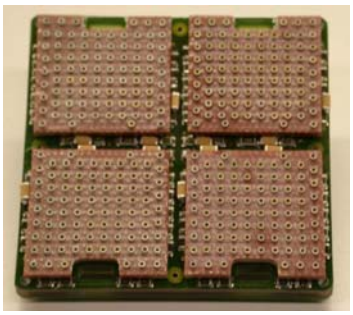

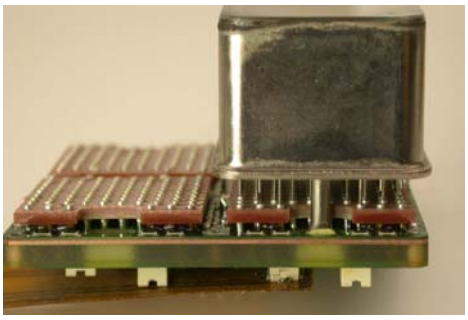

FIG. 5/a: a micro-cell base-board prototype equipped with BGA sockets
FIG. 5/b: a micro-cell base-board prototype with a MAPMT and connectors on

A group of 3 micro-cells, equipped with heaters to simulate the power dissipation of the on-board electronics, and instrumented with PT100 temperature probes, has been integrated on a PDM prototype base-plate. The assembly has then been installed on test set-up, with a cold pit at 0°C, in a geometry that kept at negligible level the convective heat exchange (see Fig. 6/a and 6/b).

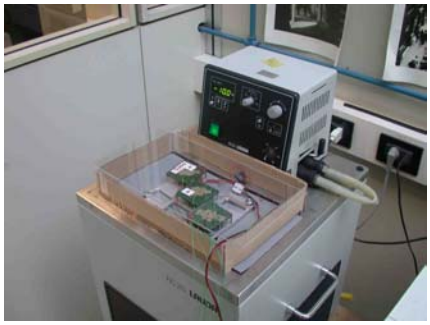

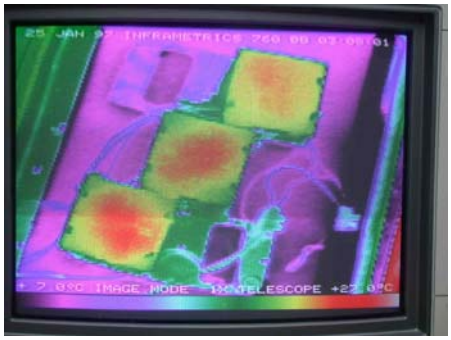

FIG. 6/a: test set-up to check heat conduction through micro-cells
FIG. 6/b: I.R. image of the micro-cells during the test

The micro-cells were connected to the base-plate with 4xM2x15 mm stainless steel screws and 3 x Φ3 x 15 mm stainless steel pins. The base-plate was kept at a temperature of 13°C, approximately uniform over its surface. The heaters have been fed so that the power dissipation on each micro-cell was about 0.27 W, that is the expected value in operation.
Base-boards surface temperature were around 22°C, slightly above room temperature, while the temperature drop measured across the mechanical links of the micro-cells ranged from 4.5 to 5.8°C. The variations were probably due to the different thermal contact between fasteners and base-board. The results are in good agreement with the simulations; the largest variations are in the base-board area, where the actual thermal resistance at the interface screw-board is difficult to be estimated a priori. The heat balance confirmed that 95% of the power was flowing through micro-cells mechanical fasteners.
Mechanical tests have been performed on a vibrating table. A support bracket has been designed and manufactured, to reproduce as much as possible the micro-cell to module interface (see fig. 7/a and 7/b).

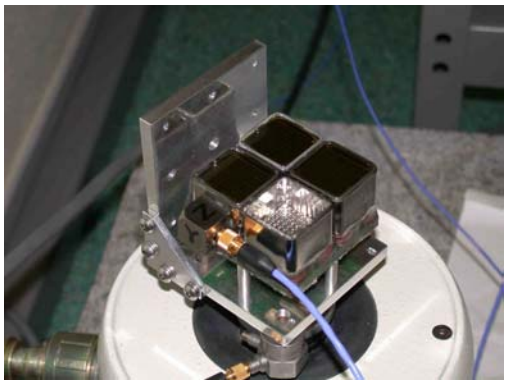

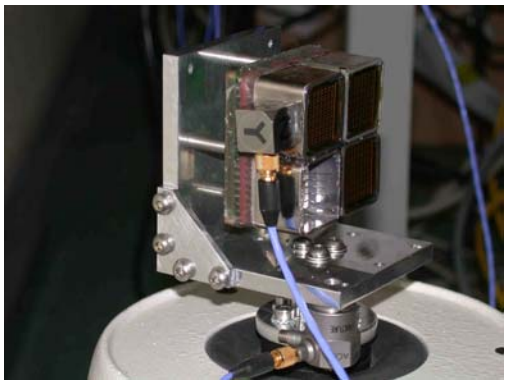

FIG. 7/a: vibrating table test set-up - micro-cell horizontal
FIG. 7/b: vibrating table test set-up - micro-cell vertical

A micro-cell sub-assembly, complete with dummy MAPMTs and potting resin, has been set up. Its measured weight, complete with screws and stainless steel spacers, was measured to be 165 gr, then much lighter than supposed in the simulations (see paragraph 1.2). There's now confidence that the final micro-cell sub-assembly, complete with chips, connectors and optical adapters, could have a total mass very close to 200 gr. The window of one of the MAPMT have been broken, to access the matrix of anodes and check electrical continuity from anode to connector on the base-board back, before and after the test.

First, the support bracket alone, equipped with a couple of accelerometers, has been submitted to a "sine sweep" from 20 to 2000 Hz, and resonances have been identified at 490/730/1480 Hz.
The micro-cell assembly has been installed, in horizontal position (see fig. 7/a), equipped with an accelerometer, and submitted to the same "sine sweep": resonances have been found at 1000 and 1300 Hz.
The Random Vibration Test has then started, submitting the assembly to "white noise" ranging from 20 to 2000 Hz; the load gradually stepped, from 4 to 9 Grms, and each step lasted 60 seconds. At last step, the spectrum measured by the accelerometer on the support bracket (input) was equivalent to 8.26 Grms.
After the RVT campaign, a sine sweep has been performed again, and resonances have been found at almost the same frequencies, as nothing had changed.
The same test campaign has been repeated with the micro-cell assembly installed in vertical position (see fig. 7/b): the resonances at 550/810/1210 Hz were about the same, before and after the test. The system has been submitted to the same "white noise", and we measured up to 8.8 Grms in input.
At the end, the assembly in horizontal position has been submitted to a "sine burst", where a sinusoidal excitation at 35 Hz and amplitude equivalent to 10.6 Grms entered the system for 10 seconds. The sine sweep again found almost the same resonances after the test. The sine burst test has been repeated with the micro-cell fastened with 3 screws only, to simulate a major failure, and again we couldn't notice any changing in the system. The micro-cell response was about the same as the input, showing a rather ineffective damping at 35 Hz.
After all the tests, the whole assembly has been inspected, and electrical continuity checked. No damage have been noticed.

2. THE PD MODULE - FIRST APPROACH

2.1 General features

The PD module is essentially an assembly where a common base-plate holds together a group of micro-cells and level 1 electronics (a digital card and a DC/DC power supply). The base-plate is then mechanically centred and secured to the focal surface global supporting structure, through 4xM8 screws and, if necessary, 2 x Φ2 mm pins, that act as both mechanical fasteners and thermal bridges.
As a starting point the PD modules have been designed to be flat, to simplify engineering and manufacturing, by flattening any region of the FS which has been selected to host one module. The dimensions of the PD modules should be compatible with the choice to flatten the PD modules, that is the actual focal surface approximation they introduce must comply with experiment general requirements. Therefore a maximum dimension of the PD module limited to about ten micro-cells was chosen.
The alternative option to leave the PD module curvature as required by the actual FS shape, more complex from the engineering point of view, can be considered if the resulting fitting to the FS is not good enough.
As a first attempt, the base-plates have been designed as made of aluminium, 6 mm thick,

that seemed to be the best compromise between mass/stiffness ratio, thermal requirements and cost implication. An alternative sandwich structure, 6 mm thick, with carbon fibre skins and aluminium honeycomb core, with glass filled PEEK inserts to house the screws, has been evaluated. It looked to be promising from the mass saving point of view, allowing a reduction to 1/3 of the aluminium base-plate mass, from 0.325 Kg to 0.100 Kg. But, on the other hand, it looked much more problematic from the thermal and economical point of views.

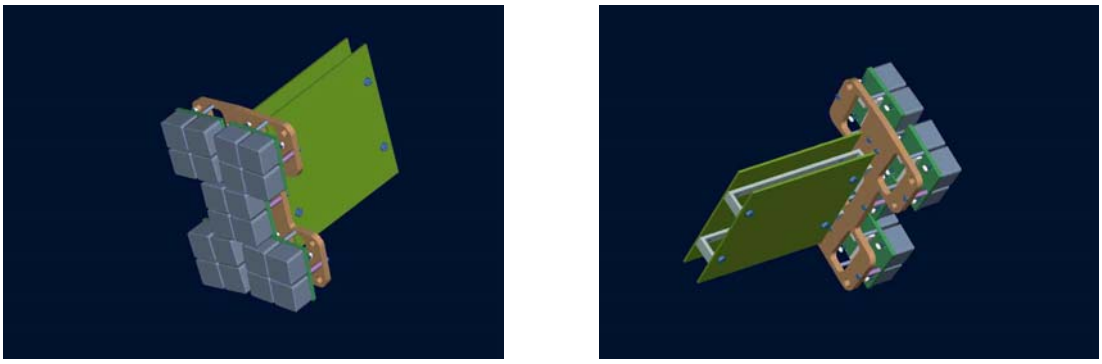

FIG. 8a/b: views of an "I" shaped module

The most complex shape of module identified in layout studies, where 5 micro-cells are arranged in a "I" footprint, has been fully CAD-modelled, to investigate implications in terms of layout and routing of the services. Even if this geometry might not correspond to the final geometry of a module, it served as an example to guide the development process. Fig. 8/a and 8/b are pictorial views of that PDM.
Module electronic cards are arranged normally to the module plane, as module width isn't large enough to house them inside its shape if arranged parallel to it. As a matter of fact, the module has been thought as an independent sub-assembly to be introduced into openings on the focal surface support structure.

2.2 Structural analysis

Static and modal analysis have been performed for both a sandwich and a single piece aluminium structure of the PD module base-plate, in the square 3 x 3 micro-cells configuration, that is one of the possible ones in any option of focal surface layout. Fig. 9 shows the meshed FEA model.

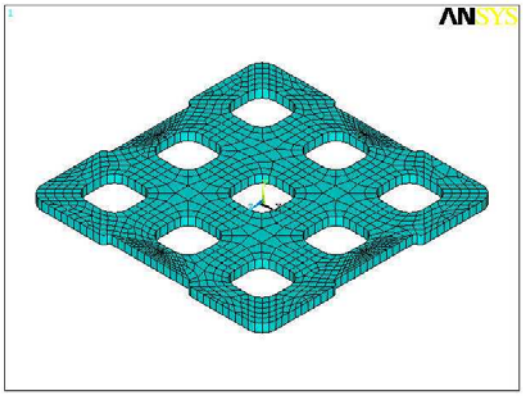

FIG. 9: FEA model of a 3x3 micro-cell module base-plate

The FEA models have been first submitted to an acceleration vector (gx,gy,gz) = (5.9g, 6.7g, 5.9g), that should reproduce the accelerations the parts will have to withstand in the Space Shuttle cargo bay during launch phase. Both aluminium massive and sandwich composite base-plates, with the mass of the micro-cells added on, showed low stress levels and deflections of the order of 0.1 mm and 0.2 mm respectively.
The modal analysis calculated, for the composite sandwich solution, a first modal frequency at 107 Hz, while, for the aluminium solution, the first calculated modal frequency was 141 Hz.
An FEA model of the complete 5-microcells "I-shaped" module has been set up, in the same configuration of the vibrating table test (see paragraph 2.4 - "Mechanical vibration of a PDM"). It must be highlighted that the micro-cell mass was around 165 gr, and that they have been modelled as fully constrained to the base-plate through 4xϕ5 mm stainless steel beams, thus assuming the M2 stainless steel screw and the coaxial aluminium spacer working as an unique beam. That configuration is much stiffer than in the previous simulations, but better compliant with test measurement, as stated below. First, an harmonic analysis have been performed between 20 and 2000 Hz, along both z-axis (normal to module plane) and y-axis (major in-plane axis of the module. Results (see spectra in Fig. 10a - 10b) highlighted a first modal frequency along z-axis at about 230 Hz, while the other modal frequencies of interest (sharp peaks) were placed between 600 and 1400 Hz. A review of the modal shapes showed that all the modes below 1400 Hz are due to baseplate motion, without significant contribution of the microcells.

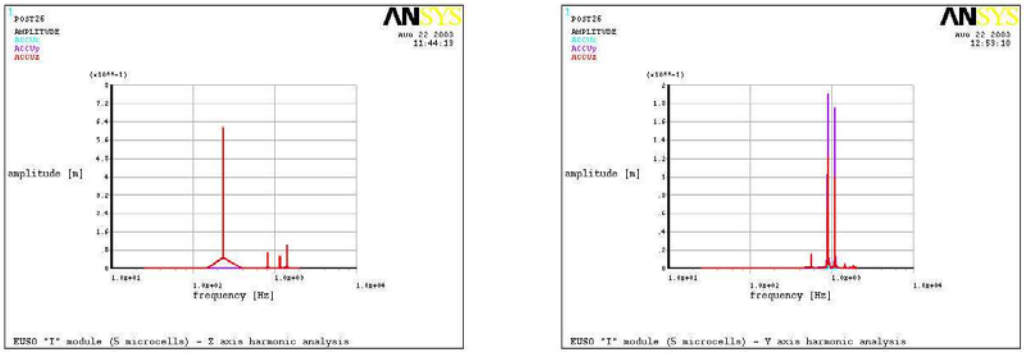

FIG. 10 a/b: harmonic analysis response spectra along Y and Z axis

Then a random vibration analysis has been performed with the input spectrum NASA suggest for qualification of items whose mass at launch is below 23 Kg [1]. Such spectrum of acceleration is equivalent to 14.1 g RMS. A standard damping ratio of 2.5% has been assumed, constant throughout the frequency range. The calculated response spectra (see Fig. 11 a/b/c) were consistent with the harmonic analysis spectra, with sharp peaks in correspondence of the modal frequencies. The integral response values, calculated on the central micro-cell as, respectively, 59.7, 62 and 46.9 gRMS along X, Y and Z-axis, were

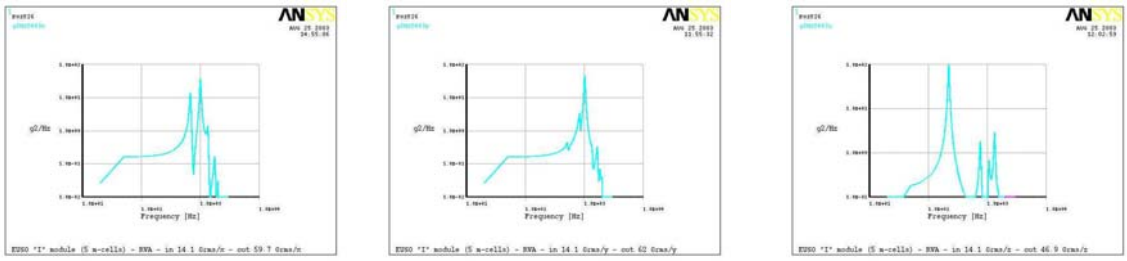

FIG. 11 a/b/c: Random Vibration Response along X, Y and Z axis respectively

rather high and indicated that the structure, as presently conceived, largely amplifies the mechanical input. The integral values, calculated on the base-plate under the central micro-cell, were respectively 52.2, 33.4, 44.2 gRMS along X, Y and Z-axis.
A cross analysis with the modal shapes highlighted that amplification through the micro-cell sub-assembly can occur not only when the excitation matches a modal frequency, but also because of merely geometrical factors. Furthermore, we noticed other micro-cell natural modes, when installed on the module base-plate, that are not calculated in the stand-alone one.
A simulation run with a 7 mm-thick (instead of 6) aluminium baseplate, that meant 30 gr mass increase (+1.9% on the PDM assembly) showed the integral response value along Y drop from 62 to 51.5 gRMS, thus proving that a stiffer baseplate could significantly improve the design.

2.3 Executive design and prototyping

To have a better feeling of the complexity related to design and manufacturing of different PDM base-plates, the one with the most complex shape coming from a possible r-φ focal surface layout have been fully designed and then manufactured. The part has been cut from an AA6082 aluminium alloy plate, with a spark-erosion process. Fig. 12/a is a picture of the item as manufactured, while Fig. 12/b shows the base-plate equipped with 3 base-boards.

FIG. 12/a: "I" shaped module base-plate prototype, as manufactured
FIG. 12/b: "I" shaped module base-plate prototype, with micro-cell base-board prototypes

Given the flat geometry, the Computer Integrated Manufacturing (CIM) approach, that allows to go directly from the CAD model to the CNC machine through an interface file, was particularly easy and convenient to apply and confirmed that the manufacturing of many differently shaped PDM base-plates shouldn't be a great issue. On the contrary, the completely different manufacturing process required by the sandwich composite solution, where a significant amount of hand work is needed to place the inserts, would have heavier cost implication if many different base-plates configurations should be produced.
Curved base-plates, though feasible, would increase the complexity of the manufacturing process. As preliminary consideration, plates bent on a mould would be easier and cheaper than milled or turned.

2.4 Laboratory tests - Mechanical Vibration of PDM

Random Vibration tests of a 5-microcells "I-shaped" PDM prototype have been performed in order to check whether some design features, as microcells fastening, are consistent with the expected flight loads. The 5-cells PDM tests features are reported in Tab.1-3 for the sine sweep, random vibration (NASA Standard qualification), and sine burst test, respectively.

Table 1. Sine Sweep (Normal mode search)

Frequency range (Hz)	20 – 2000
Scan velocity (Oct./min)	2
Amplitude (g)	0.5

Table 2. Random Vibration Spectrum

Frequency (Hz)	ADS (g^2/Hz)
20	0.026
20-50	+ 6 dB/Oct
50-800	0.16
800-2000	- 6 dB/Oct
2000	0.026
Overall	14.1 g_{RMS}
Duration	1 min

Table 3. Sine Burst

Tests level (g)	± 12.5
Frequency (Hz)	80
Duration (sec)	1

The 5-microcells PDM was equipped with a central micro-cell with four dummy MAPMTs, and four dummy masses to simulate the other micro-cells. Prototype features are reported in table 4.

Table 4. Prototype characteristics

Microcell total mass [gr]	164
Number of microcells on PDM [-]	5
Aluminium 6 mm-thick baseplate mass [gr]	188
Pb deadweight to simulate PDM electronics [gr]	495
PDM to table screws mass [gr]	97
Total PDM prototype mass [gr]	1600

The tests have been performed at the vibration facility of Galileo Avionica, with two vibration generators (Ling Dynamics System 826LS + LDS V964). The tests vibration sequences and the vibration directions are reported in Table 5.

Table 5. Test Sequences

Test Sequence	Direction
1. Normal Mode Search	Z, X
2. Random Vibration	Z, X
3. Normal Mode Check	Z, X
1. Normal Mode Search	X
2. Sine Burst	X
3. Normal Mode Check	X

The z direction is perpendicular to the PDM plane, whereas the x and y directions lie on the PDM plane. The y-axis (minor in-plane axis) was not tested assuming that, due to the 5-cells PDM geometry design, it has a behaviour very similar to the x-axis. The vibration response is monitored by two accelerometers positioned on the fixture table and on a MAPMT of the central micro-cell. The prototype setup is shown in Fig.13.

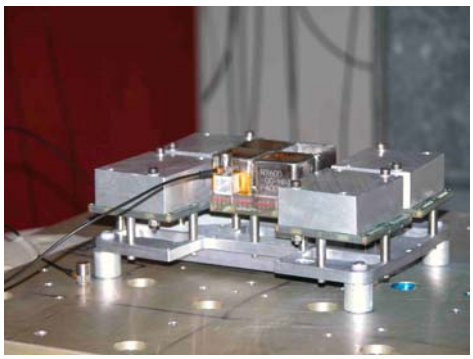

FIG. 13: Vibrating table prototype setup

The results of these preliminary vibration tests are shown in Fig. 14–15 [3)], where the response curves for the sine sweep and random vibration tests for z- and x-axis are reported

Along the vertical direction (z), the PDM has the first mode vibration at about 300 Hz, with an amplification factor Q ≈ 20, and an overall amplification in the random test from 14.1 to 39.4 g_{RMS}. The sine sweep response spectrum measured after the random vibration reproduces almost the same shape of the spectrum measured before the test.

Along the x direction, the random test amplification is the same, and the first mode vibration is at 504 Hz, with an amplification factor Q ≈ 7.6 and an overall amplification in the random test from 14.1 to 40.7 g_{RMS}. But the sine sweep response spectrum after the random vibration is slightly different, as if something changed in the PDM.

Furthermore, the sine burst test along x-axis does not affect the mode vibration pattern measured after the x-axis random vibration. It seems that random vibration settled the mechanics.

After all the tests, the whole assembly has been inspected, and electrical continuity checked from PMT to connector on micro-cell base-board backside. No damage have been noticed.

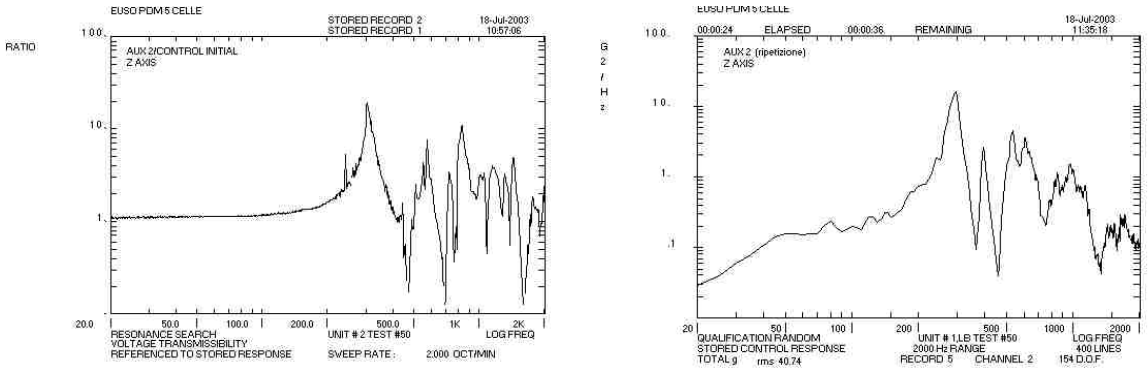

FIG. 14 a/b: Sine sweep and random vibration test response for the z (vertical) direction.

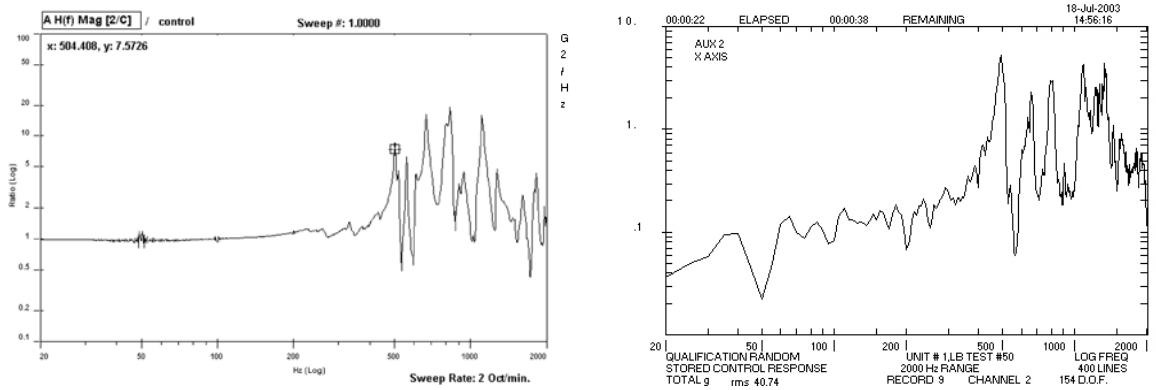

FIG. 15 a/b: Sine sweep and random vibration test response for the x (major in-plane axis) direction.

Random vibration response spectrum shapes are in relatively good agreement with the finite element simulation, but overall amplification is significantly lower, probably because actual internal damping is better then expected.
Nevertheless, the random response measured at the MAPMT level is definitely too high, compared to the level the they proved to withstand without reducing their functionality [4)].
Next module design will have to take into account of that, and yield in a stiffer and better damped behavior.
On the other hand, the microcell fastening solution (M2 stainless steel screws directly holding on the G10 microcell printed circuit board) proved to well withstand the severe load environment. They were tightened between 20 and 40 cNm and, although not equipped with lockers, none of them got loose during the tests. For future applications, 40 cNm will be assumed as the appropriate tightening torque.

3. THE PD MODULE CONCEPT REVISITED

3.1 PD module layout

After an overall budget of the detector, any possible effort has been requested towards a consistent mass reduction of all the components. Furthermore, recent developments of instrument optics defined a focal surface whose shape is noticeably far to be spherical, compared to the general geometrical accuracy requirement. Then, if a larger module allows mass saving, it must be definitely curved, to better follow the focal surface shape. All that increases, of course, the multiplicity of different types of module.
After a study of the two different detector layout options (R-φ and X-Y), a module of 20 to 25 micro-cells has been identified as the best compromise between mass reduction, modularity, complexity and multiplicity of different types of modules. Given its dimensions, such module should feature a curved, spherical base-plate.
The module should be secured to the focal surface support structure through aluminium M8 screws. The screws should be housed inside cylindrical hollow spacers, that should act also as thermal bridges. As a matter of fact, the fastening concept is the same applied to the micro-cells. The spacers should be an integral part of the focal surface support. That would allow, after measuring their actual position when the structure assembling has been completed, to re-machine them so that the modules could be oriented and follow the actual focal surface shape. This way, a correction for zero gravity environment could be introduced too.
Given the dimensions of the module, now the module electronics can be arranged parallel to the base-plate. That option must be confirmed after a detailed study of the routing of the cables.
A study of the tolerances, assuming that:

- micro-cell side length is limited to 52.9 mm overall;
- 0.5 mm as minimum installation clearance between neighbouring micro-cells, even in the worst condition;
- radial play of the micro-cell screw in module base-plate through holes: 0.1 mm;
- standard positioning accuracy of the holes on the printed circuit board (± 0.1 mm);
- standard positioning accuracy of the holes on the base-board (± 0.05 mm);

showed that the micro-cells pitch on a module can't be lower than 53.9 mm. The achievable accuracy in machining the focal surface structure will be definitely lower, given overall dimensions. Then, a larger dead area around modules should be accounted for.
Figures 16a and 16b give a pictorial view of a 5x5 module.

FIG. 16a/b: 5x5 curved module assembly

3.2 Structural analysis

The structural behaviour of a square module equipped with:

- 5x5 micro-cells with a total mass of 227 gr each, including cables, optical adapters and connectors;
- 1x5 mm thick aluminium base-plate, whose mass is 500 gr;
- 1 digital card, 150x150x2 mm, arranged parallel to the base-plate, with a total mass of 1039 gr, including cables and connectors;
- 1 DC/DC power supply card, 100x100x2 mm, parallel to the base-plate and attached to the digital card, with a total of 450 gr including cables and connectors;
- fasteners, with a total mass of 80 gr;

has been simulated by means of a finite element model. With the above-mentioned assumptions, a module would have a total mass of 7744 gr. After the experience with micro-cell prototypes, it seems that a safety margin of around 10% is included.

A preliminary calculation has been done with the module fully restrained on the screw ends at the 4 corners and 1 mm-thick module electronics cards, submitted to an acceleration vector (ax,ay,az) = (15g,15g,15g), suggested by NASA as reasonable first approach load. That first simulation identified unacceptable deformation on the module cards; a second run with card thickness increased to 2 mm and the module base restrained through 8xM8 aluminium screws on its border, showed maximum deformations limited below 3 mm, with a peak of stress on the screw to module base joint. There's confidence that, with the actual fastening with screw and spacers, the momentum will be better transferred from module to screw, and the peak will be limited below acceptable values.

A modal analysis identified the first natural frequency at 44 Hz. As expected, it is an oscillation of the module electronics. As the present preliminary design of the focal surface support structure identifies a first natural frequency at around 40 Hz [2)], probably provisions should be made to de-couple them.

Being the configuration acceptable, at least in general terms, a random vibration analysis has been performed with the input spectrum NASA suggest for qualification of items whose mass at launch is below 23 Kg [1)] (see Fig 17/a). Such spectrum of acceleration is equivalent to 14.1 g RMS. A standard damping ratio of 2.5% has been assumed, constant throughout the frequency range.

The calculated response of the system showed a sharp peak at 400 Hz (see Fig. 17/b),
when the excitation is parallel to the base-plate plane (direction x or y), with an integral value of 47.8 g RMS.

When the acceleration is orthogonal to the base-plate plane (direction z), the load configuration is slightly less demanding for the structure (see Fig. 17/c), two peaks are found at about 100 and 300 Hz, and the integral value is "only" 39.8 g RMS.

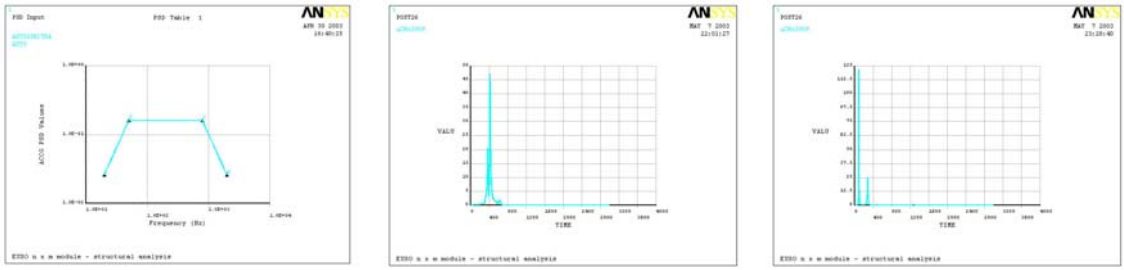

FIG. 17/a: NASA qualification spectrum equivalent to 14 gRMS
FIG. 17/b: response spectrum along X or Y, equivalent to 47.8 gRMS
FIG. 17/c: response spectrum along Z, equivalent to 39.8 gRMS

The static analysis performed with the above acceleration combined in a load vector (ax,ay,az)=(48g,48g,40g) correctly showed module to focal surface support screws working as fully constrained beams, with the most stressed points at their ends. Von Mises' equivalent stress in those points raises to peaks beyond material acceptable stress. As mentioned before, those peaks are probably related to "form effects", and there's confidence that the actual screw to base-plate joint configuration will significantly reduce them. Anyway, a different support of the module cards seems advisable, maybe through a composite, light interface frame that could limit card displacements, increase first modal frequency and better transfer the loads to module base-plate.

3.3 Thermal analysis

The thermal behaviour of a square module equipped with:

- 5x5 micro-cells with 0.31 W of waste heat on each;
- 1x5 mm thick aluminium base-plate;
- 1 digital card, 150x150x2 mm, arranged parallel to the base-plate, with 1 W of waste heat on;
- 1 DC/DC power supply card, 100x100x2 mm, parallel to the base-plate, with 2 W of waste heat on;
- 8xM8x15 aluminium screws to link the module to the focal surface support structure;

has been simulated by means of a finite element model. Radiation and conduction have been considered, assuming that:

- all surfaces have 0.85 relative emissivity (reasonable, provided that an appropriate coating is foreseen where necessary);
- ambient temperature at -15°C;
- focal surface support structure at 0°C;
- micro-cell exchange radiation only to and from the rear, that is no heat exchange occurred with experiment main optics (MAPMT front window looks like a mirror, then the assumption looks reasonable).

A first run, with both radiation and conduction active, showed that micro-cell temperature ranges between 14.5 and 17.5°C, while the maximum temperature is achieved on the DC/DC supply card (see Fig. 18/a and 18/b). Micro-cell temperature uniformity is rather good. Up to 4.5 W out of the total 10.75 W dissipated on the module flowed through module screws.

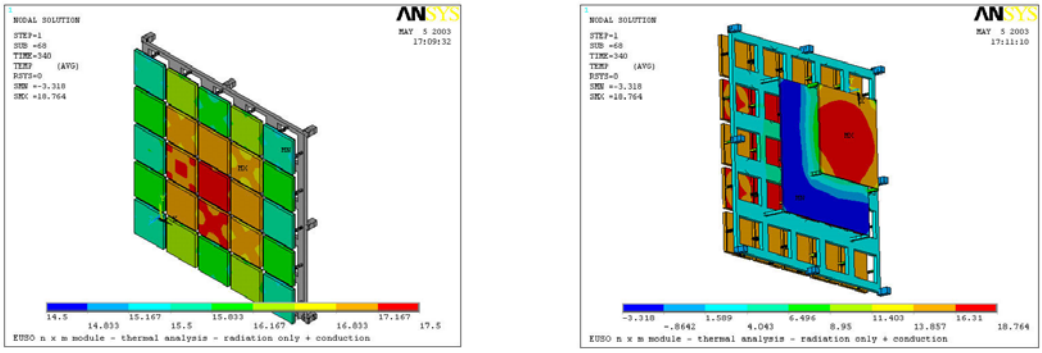

FIG. 18 a/b: temperature profile on micro-cells - both radiation and conduction are active

A second run, without any conductive heat exchange between module and focal surface supporting structure, showed an increased micro-cell temperature, that ranged between 21 and 23°C (see Fig. 19/a and 19/b).

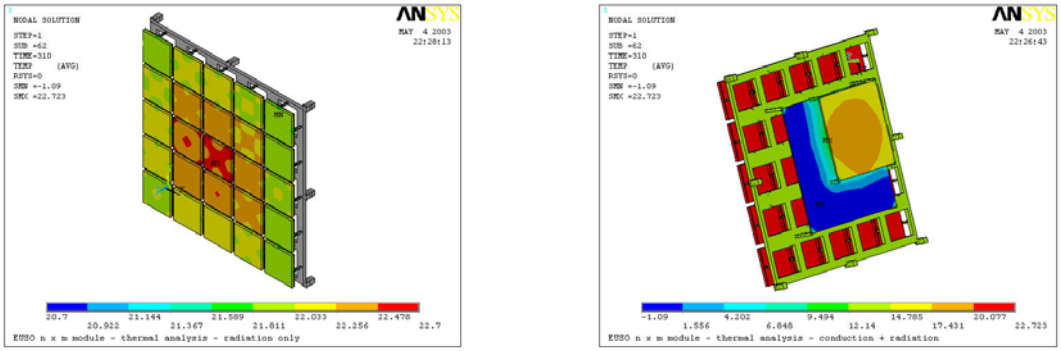

FIG. 19/a: temperature profile on micro-cells - only radiation is active

A third run has been performed with radiation only and without the 0.5 mm thick copper layer that act as heat spreader inside the micro-cells (see Fig. 20/a and 20/b).

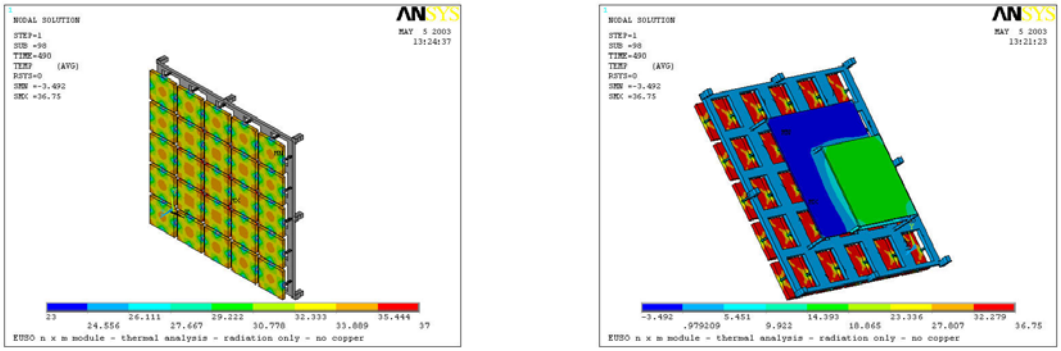

FIG. 20 a/b: temperature profile on micro-cells when only radiation is active, without copper layer inside micro-cells

That solution would allow to save around 18 Kg of mass over the whole surface, at the

price of an increased temperature on the micro-cells, that would range between 23 and 33°C.

4. CONCLUSIONS

After the R&D studies and tests performed during the EUSO "phase A", the following points can be assumed as guidelines for the final detector design:

- The micro-cell base-board design proved to be robust enough to withstand the most severe environmental conditions expected during the space mission;
- In particular, M2 stainless steel screws holding directly on a thread machined on the glass-epoxy micro-cell base-board successfully overcame all the tests and proved to be a reliable solution.
- Random vibration response is rather high, though lower than calculated. Provisions should be made to keep it below the PMT allowable limits
- The copper layer inside the micro-cell base-board can significantly reduce both temperature peaks and non-uniformities over the modules. Its thickness must be optimised, to achieve the best compromise with the mass budget

5. REFERENCES

(1) "General Environmental Verification Specification", NASA
(2) "The focal surface mechanical supporting structure", EUSO-FS-REP-003-11, Collège de France - Paris, 21/01/03
(3) "Rapporto di prova n° 278-LPA-03", Galileo Avionica, AQ/449, Campi Bisenzio (FI), 18/07/03
(4) "First/fast vibration test for EUSO PMTs", EUSO-J:005v3 - RIKEN - Japan, April 2002.
(5) "Study report on the EUSO photo-detector design", INFN / AE_01 / 04.
(6) "Il programma AirWatch ed il progetto EUSO", INFN / AE_01 / 03.